Published in final edited form as:
J Phys Chem C Nanomater Interfaces. 2007 January 18; 111(2): 981–986. doi:10.1021/jp065525d.

Electrochemical Surface Plasmon Resonance Spectroscopy at Bilayered Silver/Gold Films

Peimin Zhai[a], **Jun Guo**[a], **Juan Xiang**[a,*], and **Feimeng Zhou**[a,b,*]

[a]Institute of Surface Analysis and Biosensing, School of Chemistry and Chemical Engineering, Central South University, Changsha 410083, P. R. China

[b]Department of Chemistry and Biochemistry, California State University, Los Angeles, Los Angeles, California 90032, U. S. A.

Abstract

Bilayered silver/gold films (gold deposited on top of the silver film) were used as substrates for electrochemical surface plasmon resonance spectroscopy (EC-SPR). EC-SPR responses of electrochemical deposition/stripping of copper and redox-induced conformation changes of cytochrome *c* immobilized onto self-assembled monolayers preformed at these substrates were measured. Influence of the Ag layer thickness and the double-layer capacitance on the EC-SPR behavior was investigated. The results demonstrated that the bilayered Ag/Au metal films produce a sharper SPR dip profile than pure Au films and retain the high chemical stability of Au films. Contrary to the result by the Fresnel calculation that predicts a greater fraction of Ag in the bilayered film should result in a greater signal-to-noise ratio, the EC-SPR sensitivity is dependent on both the Ag/Au thickness ratio and the chemical modification of the surface. Factors affecting the overall SPR sensitivity at the bilayered films, such as the film morphology, potential-induced excess surface charges, and the adsorbate layer were investigated. Forming a compact adsorbate layer at the bilayered film diminishes the effect of potential-induce excess surface charges on the SPR signal and improves the overall EC-SPR sensitivity. For the case of redox-induced conformation changes of cytochrome *c*, the SPR signal obtained at the bilayered silver/gold film is 2.7 times as high as that at a pure gold film.

1. Introduction

Surface plasmon resonance (SPR)[1,2] is an optical technique that can detect adsorbates at extremely low quantities and measure infinitesimal conformation/orientation changes of the adsorbed molecules.[3–6] SPR is attractive owing to several inherent advantages (e.g., label-free analysis, simplicity, cost-effectiveness, and high sensitivity).[7–24] The SPR resonance angle variation is dependent on various physicochemical processes occurring at the SPR substrate (a thin metal film or a chemically modified metal surface) and/or the substrate/solution interface. Thus, when coupled with electrochemistry (EC-SPR), it offers a viable avenue to probe optical and electrochemical properties of adsorbates and a sensitive means to quantify thickness variations of ultrathin films accompanying redox reactions. In some cases, the SPR response can be used to decipher processes (e.g., surface adsorption vs. solution reaction) that might be difficult for voltammetric techniques to resolve. SPR resonance angles are immune to evolution of gases from certain electrolytic reactions, a process that strongly interferes voltammetric measurements.[25] Owing to these unique features, EC-SPR has emerged as a powerful coupled voltammetric technique. For example,

Corresponding authors. Tel: 323-343-2390. Fax: 323-343-6490. fzhou@calstatela.edu (F. Zhou) and xiangj@mail.csu.edu.cn (J. Xiang).

Knoll and co-workers coupled EC in-situ with SPR to investigate the electrochromic and redox switching properties of conductive polymer and copolymer thin films.[26,27] Kang et al. studied the electropolymerization of aniline and doping/dedoping processes in polypyrrole films.[28–30] Szunerits and coworkers used an imaging SPR to follow the microarray patterning process aided by electropolymerization of pyrrole-labeled oligonucleotides.[31,32] Imaging SPR had also been used in tandem with voltammetry to characterize micropatterned lipid membranes.[33] Tao and co-workers combined cyclic voltammetry with a multiwavelength SPR to determine conformational and electronic changes of cytochrome *c*.[34] Our group quantified the orientation changes of ferrocenyl alkanethiol self-assembled monolayers (SAMs) upon electrochemical oxidation of the ferrocene termini.[35] To alleviate the effect of an applied potential on the SPR response, we electrochemically induced local structural changes with redox species generated at a scanning electrochemical microscopic tip electrode and simultaneously determined such changes using a highly sensitive SPR.[36] These examples demonstrate that, when used in tandem with a voltammetry-based technique, SPR is quite useful for probing phenomena and processes at thin film/solution interfaces.

In general, the dependence of the SPR angular shift ($\Delta\theta_R$) on an externally applied electrode potential (ΔV) is predominantly governed by the three factors in the following equation:[4]

$$\frac{\Delta\theta_R(\lambda)}{\Delta V}=c_1\frac{\Delta n(\lambda)}{\Delta V}+c_2\frac{\Delta d}{\Delta V}+c_3\frac{\Delta\sigma}{\Delta V} \quad (1)$$

where Δn, Δd, and $\Delta\sigma$ are changes in the refractive index, average thickness of the adsorbed molecular layer, and the surface charge density of the electrode, respectively. c_1, c_2 and c_3 are constants and λ is the wavelength of the incident light. The third term in equation 1 suggests that a change of surface charge density of the electrode resulted from the variation of the applied potential will shift the resonance angle. Based on the free electron model of metals,[37] Kötz et *al.* proposed that an externally applied potential could change the dielectric constant of the metal film by altering the free electron density.[38] Using a 50-nm-thick silver film as an example, Tao and co-workers found via a theoretical calculation[4] and experimental measurements[39] that ΔV of 1 volt could induce an angular shift as large as 0.02°. Such a change is several times greater than commonly observed SPR angular shifts caused by conformational change of organic or even biological adsorbates.[36] Because the excess surface charges introduce a large background, measuring tiny changes originated from electrochemical reactions could become difficult for EC-SPR. Even for changes that are sufficiently large, a background subtraction procedure has to be implemented. Unfortunately, in many cases there is a lack of suitable substrates that closely mimic the surface of interest in terms of their chemical property and structure for a reliable background subtraction procedure.[36]

One approach to mitigate the above problem is to reduce the effect of the applied electrode potential on the variation of the surface charge density (i.e., noise reduction). For example, chemically modifying the substrate surface can reduce the double-layer capacitance of the substrate and consequently decrease the excess surface charge.[40] By self-assembling alkanethiol molecules on silver films, Wang et al. demonstrated that the SPR angular shift in response to the potential modulation is linearly proportional to the reciprocal alkanethiol chain length.[41] Another approach is to design new instrumental setups or develop novel SPR substrates to enhance the small SPR responses (i.e., signal enhancement). Uses of a waveguide,[42,43] a double-wavelength detection scheme,[14] and a bicell detector[23,24,39] are just a few examples that have been shown to be effective in improving SPR measurements. As far as the fabrication of novel SPR substrates is concerned, porous active phases,

nanocrystals, and nanoparticles have been demonstrated to be suitable candidates.[44–46] Mirsky and co-workers were the first to fabricate bimetallic silver/gold layers as substrates for chemical and biological sensing with SPR, wherein the gold layer was in contact with the sample solution.[13] The sharp and intense SPR resonance peak (dip) of the Ag underlayer[3] improved the sensitivity of the resultant sensors and the high stability of the Au overlayer retains the chemical inertness of the sensor surface.[13,47] Thus it is conceivable that the thicker the Ag underlayer, the greater the sensitivity.

Since fabrication of these bilayered Ag/Au films is straightforward, the exploration of them as substrates for EC-SPR could be useful for measurements of small SPR signal variations triggered by electrochemical reactions. Through EC-SPR studies of electrodeposition/anodic stripping of copper and redox-induced conformation changes of cytochrome *c*, we show that the Ag underlayer leads to an enhancement of SPR signal over a pure Au film, while the Au overlayer is robust and offers a wide potential range for voltammetric studies. Interestingly, unlike the use of such substrates for chemical and biological sensing wherein a thicker Ag underlayer would be more favorable, the extent of signal enhancement is dependent on the surface property of the Au overlayer and the Ag/Au thickness ratio. In this work, influences of the thickness of the Ag underlayer and the morphology and surface modification of the Au overlayer on the EC-SPR response were investigated and delineated with the free electron model of metals.

2. Experimental Methods

Chemicals and Materials

Sulfuric acid and $CuSO_4$ (Beijing Reagent Co.) were of reagent grade and used as received. 11-mercaptoundecanoic acid (MUA) and hexanethiol (HT) were obtained from Aldrich (Milwaukee, WI). Cytochrome *c* (cyt c) was acquired from Sigma Chemical Co. (St. Louis, MO). All solutions were prepared with deionized water (Milli-Q, Millipore Corp).

Electrodes and Cell

A PEEK electrochemical cell (Biosensing Instruments, Tempe, AZ) was used for all EC-SPR experiments. Au or bilayered Ag/Au films were used as the SPR substrates and the working electrodes. The area of the film exposed to the electrolyte solution is approximate 0.45 cm^2. An Ag/AgCl and a platinum wire were used as the reference and auxiliary electrodes, respectively.

Instruments

SPR measurements were carried out with a BI 1000 SPR system (Biosensing Instruments). To conduct SPR simultaneously with electrochemistry, the SPR instrument, connected to a CHI 660 electrochemical workstation (CH Instruments, Austin, TX) via a coaxial cable, inputs the potential and current values measured by the electrochemical workstation through an interface card.

Preparation and Modification of the Bilayered Metal Substrates

BK7 glass slides (Fisher Scientific, Tustin, CA) were heated in piranha solution (30% H_2O_2 and 70% concentrated H_2SO_4) at 80°C for 30 min. Upon cooling to room temperature, the glass slides were thoroughly cleaned with water and sonicated in a solution of H_2O:NH_4OH:30%H_2O_2 (V:V:V = 5:1:1) for 60 min. After rinsing the surface with water and drying under a N_2 steam, 2-nm-thick Cr underlayers were deposited onto the slides using a sputter coater (Cressington model 108SE, Ted Pella, Inc., Redding, CA) modified by incorporating a F-100/110 turbo molecular pump (Zhongke Instruments, Beijing). This step was followed by depositing Ag and Au layers in series with desired thicknesses. The total thickness of the

two layers was kept at 50 nm. For the cyt *c* film formation, a MUA SAM was first attached to the surface by immersing the bilayered film in 2.0 mM MUA for 18 h. The MUA-covered film was then submerged in a 50 mM phosphate buffer (pH 7.0) containing 10 μM cyt *c* for 2 min. Au films covered with cyt *c* were prepared in the same manner.

Characterization of the Bilayered Metal Substrates

The surface morphology of the bilayered metal substrates was examined using both a LEO1530 scanning electron microscope (LEO Co., Germany) and an atomic force microscope (Model Pico-plus, Molecular Imaging, Tempe, AZ). To estimate the roughness of the substrates, HT SAMs were first formed by immersing the substrates in 2.0 mM HT for 18 h. The as-prepared HT SAMs were then reductively desorbed in 0.5 M KOH. Amounts of HT desorbed electrochemically were compared to the result expected at an atomically flat Au substrate[48,49] to yield average roughness values.

3. Results and Discussion

One of the SPR detection modes measures the resonance angle shift. Understandably, a steeper and sharper reflectivity curve (SPR dip profile) would afford higher resolution and a greater signal-to-noise ratio. In addition, it is known that the electromagnetic (evanescent) wave propagating into the solution phase is also dependent on the type of metal films.[3] For example, the penetration length of a 50-nm-thick Au film is about 164 nm with a light source of 630 nm, whereas that of a 50-nm-thick Ag substrate is about 219 nm.[3,50] It is thus apparent that SPR originated from an Ag-based film will be capable of probing interfacial processes at a greater distance. Figure 1a displays a series of reflectivity curves for various Ag/Au thickness ratios based on the Fresnel calculation. For clarity, we plotted the peak width (φ) at a constant reflectivity value (0.1 or 10% reflectivity chosen in the present case) as a function of the Ag/Au thickness ratios. Evidently, the peak width inversely increases with the Ag/Au thickness ratio. Thus the Fresnel calculation indicates that the insertion of an Ag layer between the glass slide and the gold overlayer should improve the SPR resolution. We should note that, in the Fresnel calculation, the effect of an externally applied potential on the SPR resonance curve[34,38] was not considered. As will be discussed in connection with the description of our EC-SPR results, the externally applied potential and the interfacial property of the metal substrate both contribute to the overall SPR resonance angle change, making the experimental results deviate from the Fresnel calculation.

Previously, Jung et al. used SPR in conjunction with anodic stripping voltammetry for trace metal analysis.[51] We therefore used electrodeposition/anodic stripping of copper as a model system to compare the voltammetric and SPR responses at the bilayered film to those at a pure Au film. Figure 2 is an overlay of cyclic voltammograms (CVs, panel a) acquired at an Ag/Au bilayered metal film (solid line curve) and an Au film (dotted line curve) in a solution of 5 mM $CuSO_4$/0.1 M H_2SO_4, together with the simultaneously recorded SPR dip shifts (panel b). As can be seen, during the cathodic scan, Cu^{2+} was reduced (cathodic peak potential $E_{pc} = -0.07$ V) and deposited as Cu onto the surface. At the same time, the net SPR dip shift was positive, meaning that the deposited Cu film had increased the overall SPR angle. During the reverse scan, the deposited copper could be completely desorbed (anodic peak potential $E_{pa} = 0.16$ V), which caused the SPR angle to return to the original value (i.e., overall dip shift was negative). As can be seen, the voltammograms at the two different types of films are almost congruent, indicating that the morphology and chemical property of the Au overlayer in the bilayered Ag/Au film are essentially identical to those of the pure Au film. However, the bilayered film produced a greater SPR dip shift at the potential when Cu is deposited than the Au film (panel b), due to the sharper SPR dip profile inherent in the Ag underlayer.

We also assessed the quantitative aspect of the EC-SPR measurement of the amount of copper deposited. Integrating charges under the reduction peaks in Figure 2a yielded the thickness of the deposited copper film to be approximately 13 nm for both types of substrates. Based on the Fresnel equation and a five-layer (glass/Ag/Au/Cu/H_2O) model for the SPR signal at the bilayered Ag/Au substrate and a four-layer (glass/Au/Cu/H_2O) model for the pure Au substrate (Figure 1b), the thicknesses of the copper films at the two substrates were both found to be 15 nm. In performing the Fresnel calculation, we used 0.27 + 3.42i as the complex refractive index for Cu[52]. Such an excellent agreement between the electrochemical result and the calculated SPR value indicates that EC-SPR can provide an accurate measurement of thickness variation of an adsorbate or a deposited film with known refractive indices. Moreover, the voltammograms and the SPR dip-potential diagrams can also be used to gauge the quality of the bilayered films. If the Ag layer is not completely covered by the top Au film, the bilayered film will produce irregular voltammograms and unpredictable SPR dip-potential diagrams. We found that, when the Ag/Au thickness ratios were at or less than 1/1, more than 80% of the sputter-coated bilayered substrates were highly robust and could be used in repeated EC-SPR experiments without appreciable signal degradation. The substrate stability deteriorates slightly for films with the Ag/Au thickness ratios greater than 1/1.

To better represent the signal enhancement, we use the following coefficient *Q*:

$$Q = \Delta\theta_{Ag/Au} \Big/ \Delta\theta_{Au} \tag{2}$$

where $\Delta\theta_{Ag/Au}$ and $\Delta\theta_{Au}$ correspond to the maximal SPR signals associated with Cu^{2+} electroreduction at the Ag/Au substrate and at the Au substrate, respectively. Figure 3 is a plot of *Q* vs. the Ag/Au thickness ratio. The results suggest that the highest EC-SPR signal is achieved at the Ag/Au thickness ratio of 1/3. At this thickness, the maximal SPR signal intensity at the bilayered film is 1.3 times as high as that at a pure Au film. The parabolic relationship is somewhat surprising, since the Fresnel calculation (cf. Figure 1) predicts that the SPR signal should increase with the thickness of the Ag underlayer. In fact, when the Ag/Au ratio exceeds 1/1, the *Q* value is essentially equal to 1.

Two possible factors may contribute to the deviation of the observed signal enhancement from the theoretical prediction. First, the compactness and uniformity of the Ag underlayer are dependent on its thickness and can affect the morphology or structure of the Au overlayer. Panels a–c in Figure 4 are the SEM images of 10.0-, 12.5-, and 16.7-nm thick Ag films, respectively. These values correspond to the Ag underlayers in the bilayered films with the Ag/Au ratios of 1/4, 1/3, and 1/2, respectively. A close comparison of the three images reveals that only the 10-nm-thick Ag film possesses distinctly different and large grains. There is virtually no appreciable difference in morphology or structure between the 12.5- and the 16.7-nm-thick films. These similar Ag surfaces suggest that the Au layers on top should have comparable roughness. Cross-sectional contour analyses of AFM images of the bilayered Ag/Au substrates with 12.5- and 16.7-nm-thick Ag underlayers (not shown) and a pure Au film showed highly comparable morphologies. For example, the roughness values of a bilayered Ag/Au substrate with a thickness ratio of 1/2 and a pure Au film are 5.2 ± 0.2 nm and 4.7 ± 0.3 nm, respectively. These values are also in good agreement with those estimated from amounts of HT SAM reductively desorbed off a bilayered Ag/Au film (~7.6 nm) and a pure Au film (~5.9 nm). Since these values are not much smaller than 10 nm (i.e., the thickness of the Ag film in Figure 4a), an Ag underlayer of 10 nm or less would not produce bilayered Ag/Au substrates with a relatively smooth morphology. Note that such a thickness is inconsequential for the EC-SPR signal enhancement, because a very thin

Ag layer would not be favorable for a high *Q* value. Taken all these observations into account, it becomes understandable why the voltammetric behavior of the bilayered film (Figure 2a), which is solely governed by the structure and property of the Au overlayer, is comparable to that of a pure Au film. The morphological effect becomes important only when the Ag underlayer is very thin.

The second effect is that the potential-induced excess charges at the SPR metal film may cause the deviation from the Fresnel calculation. Kötz et *al.* showed that an externally applied potential could change the dielectric constant of the metal film,[38] ε_m, by altering the free electron density, n_e, according to the free electron model of metals:[37]

$$\varepsilon_m(\omega)=1-\frac{n_e e^2}{\varepsilon_0 m_e \omega^2} \tag{3}$$

where e, m_e, and ω are the electronic charge, electronic mass, and frequency of light, respectively. The effect of the potential-induced excess surface charge Δn_e on the change of dielectric constant ($\Delta\varepsilon_m$) is given by:

$$\Delta\varepsilon_m=(\varepsilon_m-1)(\Delta n_e/n_e) \tag{4}$$

and the relationship between the excess surface charge and the interfacial property of the metal film is:

$$\Delta n_e=-C_{dl}\Delta V/ed_m \tag{5}$$

where d_m is the thickness of the metal film and C_{dl} is the double-layer capacitance.

Based on equations 1, 4, and 5, $\Delta\theta \propto \Delta\boldsymbol{\sigma} \propto \Delta\boldsymbol{\varepsilon}_m \propto \Delta V$. Thus, the magnitude of the proportionality constant between Δθand ΔV will be determined by the values of C_{dl} and d_m. If C_{dl} remains constant, the potential(or excess surface charge)-induced SPR dip shift is mainly affected by the thickness of the metal film. To examine this relationship, we performed a series of potential scans at the bilayered Ag/Au films of various thickness ratios. As shown in Figure 5, the observed SPR dip shifts (Δθ) are indeed proportional to the applied potential (ΔV). As the thickness of the Au overlayer decreases, the dependence of Δθ on ΔV becomes more pronounced. Thus, it is clear that for the given electrolyte solution and within the Ag/Au thickness ratios studied, variation of C_{dl} at the Au film/solution interface is insignificant. C_{dl} is largely affected by the electrode structure (i.e., crystallinity and morphology), nonspecific adsorption of ions, and specific adsorption of analytes or impurities.[40] As discussed above, as long as the thickness the Ag underlayer is greater than 10 nm, the surface structure of the Au overlayer should be independent of the Ag film thickness. Moreover, because all the curves in Figure 5 were recorded in the same electrolyte solution, nonspecific and specific adsorptions should be analogous. Therefore, the plot in Figure 3 is consistent with the trend predicted by the relationship derived from equations 1, 4, and 5. Therefore, in using the bilayered Ag/Au films for enhanced EC-SPR measurements, a judicious choice of the thickness ratio needs to be made. Contrary to the bilayered films used for conventional SPR (bio)affinity measurements,[13] a high Ag/Au thickness ratio will augment the effect of the excess surface charge on the SPR dip shift and decrease the EC-SPR signal/noise ratio.

It is well known that an adsorbate layer at an electrode decreases the double-layer capacitance, since the distance of the locus of counter ions from the electrode will be

increased by the thickness of the adlayer.[53] Based on equation 5, the dependence of the excess surface charge on the thickness of the Au overlayer will be consequently attenuated. In fact, scanning potential at a MUA-modified Au film and a MUA-covered Ag/Au bilayer with a thickness ratio of 1/3 showed little difference in the corresponding SPR shift-potential diagrams. To demonstrate that a decrease in the double-layer capacitance would eventually lead to a greater *Q* value, we immobilized cyt *c* onto MUA SAMs preformed at bilayered Ag/Au films of different thickness ratios and then conducted EC-SPR experiments. Figure 6a is an overlay of CVs of an MUA-covered Au film (dotted black curve) and cyt *c* molecules immobilized onto MUA films preformed onto an Au film (red curve) and bilayered Ag/Au films of two different thickness ratios (blue and black curves). The correspondingly SPR shift-potential diagrams are displayed in panel b. Notice that the current density values in Figure 6a are much smaller than those in Figure 2a. This is understandable since the values in Figure 6a arose from redox reactions of molecules with monolayer or sub-monolayer coverage, whereas those in Figure 2a are associated with deposition of a much thicker and denser metal film. As can be seen, the voltammograms of cyt *c* are highly comparable, indicating that amounts of adsorbed cyt *c* molecules at and their molecular orientations with respect to the different substrate surfaces are similar. This again confirms that the morphologies of the pure Au and the bilayered Ag/Au films are comparable. A *Q* value of 2.7 was deduced upon comparing the steady-state values in the black and red curves in panel b. Such a value is greater than the highest *Q* value for the copper electrodeposition/anodic stripping experiment (cf. Figure 3) at an unmodified Ag/Au bilayer. Moreover, the quantitative aspect of the SPR dip-potential diagrams at the bilayered Ag/Au substrates is excellent. Substituting n(MUA) = 1.45, d(MUA) = 1.7 nm, and n (cyt *c*) = 1.5 into the Fresnel equation and using the known redox-induced cyt *c* conformation change ($\Delta n = 0.3$ nm)[34,36], we calculated the dip shift at a pure Au film to be 0.006°. The same calculation for the dip shift at the bilayered Ag/Au film with a thickness ratio of 1/2 produced a value of 0.015°. These values are very close to the experimentally measured values (cf. the red and solid black curves in Figure 6b) and correspond to a signal enhancement factor of 2.5. Thus, it is clear that, in line with the prediction by equation 5, the decreased double-layer capacitance alleviates the effect of excess surface charge on the SPR background signal and forming an adsorbate layer at the bilayered Ag/Au films is an effective way to further enhance the SPR signal.

4. Conclusions

Bilayered silver/gold metal films were explored as substrates for sensitive EC-SPR measurements. Our results demonstrated that such a bilayered film yields a sharper or narrower SPR dip profile than a pure Au film, whereas the Au overlayer provides a wider potential range than an Ag film for voltammetric experiments. We found that there is an intricate relationship between the Ag/Au thickness ratio and the observed SPR signal enhancement. Contrary to the Fresnel predication, which shows that a thicker Ag film should increase the SPR signal-to-noise ratio, the highest EC-SPR signals are achieved with a moderate Ag/Au thickness ratio. For unmodified bilayered Ag/Au films, a ratio of 1/3 leads to an enhancement factor of 1.3. However, this enhancement factor can be much augmented by chemically modifying the surface of the bilayered substrate (i.e., the Au overlayer) with a compact film. This enhancement is due to the reduction of the effect of the potential-induced excess surface charge on the SPR response (i.e., noise reduction). For cyt *c* immobilized on top of a preformed MUA SAM, an enhancement factor of 2.7 can be obtained. This is significant given that the excess surface charge created by the applied electrode potential has limited the applications of SPR for studying electrode reactions at a very sensitive level. The implication of this work is that the thickness of the Au overlayer and Ag underlayer and the modification of the topmost metal layer are all essential parameters for striving for the best EC-SPR signal/noise ratio.

Acknowledgments

We thank Mr. Bin Liu for his help on the fabrication of the substrates. This work was partially supported by the National Natural Science Foundation (20503040 and 20225517), the Cultivation Fund of the Ministry of Education of China (704036), a NSF-RUI grant (0555224) and a NIH SCORE subproject (GM 80101).

References

1. Otto A. Z. Phys. 1968; 216:398–407.
2. Kretschmann E. Z. Phys. 1971; 241:313–324.
3. Hanken, DG.; Jordan, CE.; Frey, BL.; Corn, RM. Electroanalytical Chemistry: A Series of Advances. Bard, AJ.; Rubenstein, I., editors. Vol. Volume 20. New York: Marcel Dekker; 1998. p. 141-226.
4. Wang, S.; Boussaad, S.; Tao, NJ. Surfactant Sci. Ser. Rusling, JF., editor. Vol. Vol. 111. New York: Marcel Dekker; 2003. p. 213-251.
5. Karlsson R. J. Mol. Recognit. 2004; 17:151–161. [PubMed: 15137023]
6. Cooper MA. Anal. Bioanal. Chem. 2003; 377:834–842. [PubMed: 12904946]
7. Piscevic D, Lawall R, Vieth M, Liley M, Okahata Y, Knoll W. Appl. Surf. Sci. 1995; 90:425–436.
8. Rothenhäusler B, Knoll W. Nature. 1998; 332:615–617.
9. Nelson BP, Grimsrud TE, Liles MR, Goodman RM, Corn RM. Anal. Chem. 2001; 73:1–7. [PubMed: 11195491]
10. Goodrich TT, Lee HJ, Corn RM. J. Am. Chem. Soc. 2004; 126:4086–4087. [PubMed: 15053580]
11. Phillips KS, Han JH, Martinez M, Wang Z, Carter D, Cheng Q. Anal. Chem. 2006; 78:596–603. [PubMed: 16408945]
12. Phillips KS, Wilkop T, Wu JJ, Al-Kaysi RO, Cheng Q. J. Am. Chem. Soc. 2006; 128:9590–9591. [PubMed: 16866487]
13. Zynio SA, Samoylov AV, Surovtseva ER, Mirsky VM, Shirshov YM. Sensors. 2002; 2:62–70.
14. Zybin A, Grunwald C, Mirsky VM, Kuhlmann J, Wolfbeis OS, Niemas K. Anal. Chem. 2005; 77:2393–2399. [PubMed: 15828772]
15. Gotoh M, Hasebe M, Ohira T, Hasegawa Y, Shinohara Y, Sota H, Nakao J, Tosu M. Genet. Anal.: Biomol. Eng. 1997; 14:47–50.
16. Sawata S, Kai E, Ikebukuro K, Iida T, Honda T, Karube I. Biosens. Bioelectron. 1999; 14:397–404. [PubMed: 10422241]
17. He L, Musick MD, Nicewarner SR, Salinas FG, Benkovic SJ, Natan MJ, Keating CD. J. Am. Chem. Soc. 2000; 122:9071–9077.
18. Lahiri J, Isaacs L, Tien J, Whitesides GM. Anal. Chem. 1999; 71:777–790. [PubMed: 10051846]
19. Ostuni E, Chapman RG, Holmlin RE, Takayama S, Whitesides GM. Langmuir. 2001; 17:5605–5620.
20. Jung LS, Campbell CT, Chinowsky TM, Mar MN, Yee SS. Langmuir. 1998; 14:5636–5648.
21. Shumaker-Parry JS, Campbell CT. Anal. Chem. 2004; 76:907–917. [PubMed: 14961720]
22. Whelan RJ, Wohland T, Neumann L, Huang B, Kobilka BK, Zare RN. Anal. Chem. 2002; 74:4570–4576. [PubMed: 12236371]
23. Song F, Zhou F, Wang J, Tao N, Lin J, Vellanoweth R, Morquecho Y, Wheeler-Laidman J. Nucleic Acids Res. 2002; 30:e72. [PubMed: 12136120]
24. Yao X, Li X, Toledo F, Zurita-Lopez C, Gutova M, Momand J, Zhou F. Anal. Biochem. 2006; 354:220–228. [PubMed: 16762306]
25. Abanulo JC, Harris RD, Bartlett PN, Wilkinson JS. Appl. Opt. 2001; 40:6242–6245. [PubMed: 18364928]
26. Baba A, Lubben J, Tamada K, Knoll W. Langmuir. 2003; 19:9058–9064.
27. Wang Y, Knoll W. Anal. Chim. Acta. 2006; 558:150–157. [PubMed: 17723433]
28. Kang X, Jin Y, Cheng G, Dong S. Langmuir. 2002; 18:1713–1718.
29. Kang X, Jing Y, Cheng G, Dong S. Langmuir. 2002; 18:10305–10310.

30. Damos FS, Luz RCS, Kubota LT. Electrochim. Acta. 2006; 51:1304–1312.
31. Fortin E, Defontaine Y, Mailley P, Livache T, Szunerits S. Electroanalysis. 2005; 17:495–503.
32. Szunerits S, Knorr N, Calemczuk R, Livache T. Langmuir. 2004; 20:9236–9241. [PubMed: 15461512]
33. Wang Z, Wilkop T, Cheng Q. Langmuir. 2005; 21:10292–10296. [PubMed: 16262279]
34. Boussaad S, Pean J, Tao NJ. Anal. Chem. 2000; 72:222–226. [PubMed: 10655657]
35. Yao X, Wang J, Zhou F, Wang J, Tao N. J. Phys. Chem. B. 2004; 108:7206–7212.
36. Xiang J, Guo J, Zhou F. Anal. Chem. 2006; 78:1418–1424. [PubMed: 16503589]
37. Kittle, C. Solid State Physics. New York: John Wiley & Sons, Inc.; 1996.
38. Kötz R, Kolb DM, Sass JK. Surf. Sci. 1977; 69:359–364.
39. Tao NJ, Boussaad S, Huang WL, Arechabaleta RA, D'Agness J. Rev. Sci. Instrum. 1999; 70:4656–4660.
40. Bard, AJ.; Faulkner, LR. Electrochemical Methods: Fundamentals and Applications. 2nd Ed.. New York: John Wiley & Sons; 2001.
41. Wang S, Boussaad S, Wong S, Tao NJ. Anal. Chem. 2000; 72:4003–4008. [PubMed: 10994957]
42. Slavik R, Homola J, Ctyroky J, Brynda E. Sens. Actuators. 2001; B 74:106–111.
43. Stamm C, Dangel R, Lukosz W. Opt. Commun. 1998; 153:347–359.
44. Hutter E, Fendler JH, Roy D. J. Phys. Chem. B. 2001; 105:11159–11168.
45. Lyon LA, Musick MD, Natan MJ. Anal. Chem. 1998; 70:5177–5183. [PubMed: 9868916]
46. Uchida K, Otsuka H, Kaneko M, Kataoka K, Nagasaki Y. Anal. Chem. 2005; 77:1075–1080. [PubMed: 15858988]
47. Sharma AK, Gupta BD. Nanotechnology. 2006; 17:124–131.
48. Walczak MM, Popenoe DD, Deinhammer RS, Lamp BD, Chung C, Porter MD. Langmuir. 1991; 7:2687–2693.
49. Weisshaar DE, Lamp BD, Porter MD. J. Am. Chem. Soc. 1992; 114:5860–5862.
50. Ordal MA, Long LL, Bell RJ, Bell SE, Bell RR, Alexander JRW, Ward CA. Appl. Opt. 1983; 11:1099–1119. [PubMed: 18195926]
51. Jung CC, Saban SB, Yee SS, Darling RB. Sens. Act. B. 1996; 32:143–147.
52. Johnson PB, Christy RW. Phys. Rev. B. 1972; 6:4370–4379.
53. Finklea, HO. Electroanalytical Chemistry. Bard, AJ.; Rubinstein, I., editors. Vol. Vol. 19. New York: Marcel Dekker; 1996. p. 109-335.

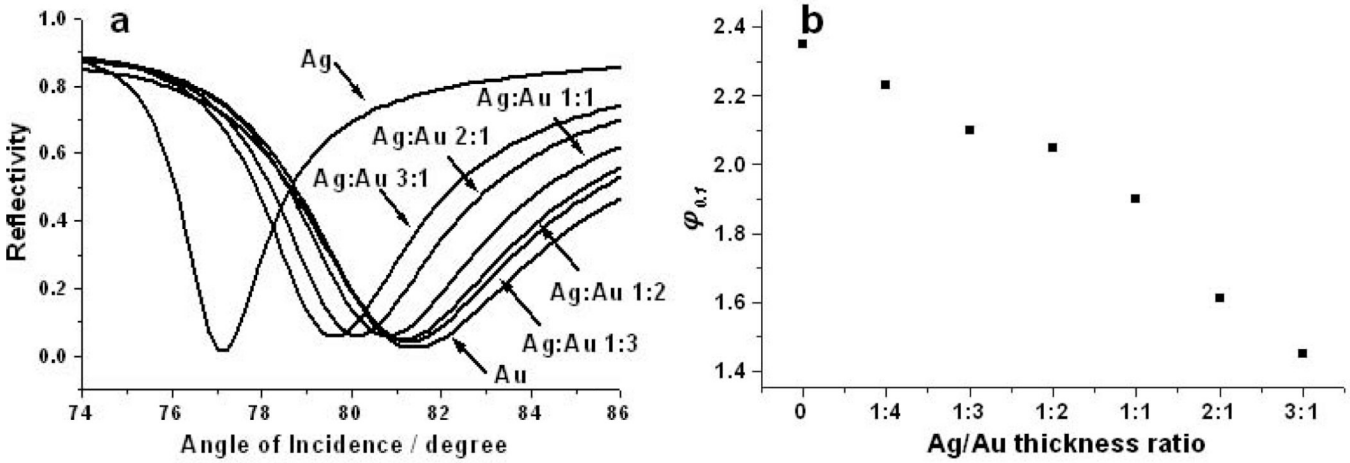

Figure 1.

SPR reflectivity curves for various Ag/Au thickness ratios determined from complex Fresnel calculations (a) and correlation of the peak width $\varphi_{0.1}$ versus the Ag/Au thickness ratio (b). The total thickness of the bilayered film was 50 nm. The following values, similar to those determined experimentally, were used for the calculations: $n_{prism} = 1.515$, $n_{Au} = 0.154 + 3.55i$, $n_{Ag} = 0.07 + 4.05i$, $n_{H2O} = 1.3$, and the wavelength of light was 632.8 nm.

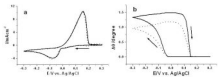

Figure 2.

Cyclic voltammograms (a, solid line curve) and the simultaneous SPR dip shifts (b, solid line curve) acquired in a 5 mM $CuSO_4$/0.1 M H_2SO_4 solution at a bilayered film with a Ag/Au thickness ratio of 1/3. The same measurements were conducted at a 50-nm thick Au film (dotted line curve in both panels). The scan rate was 50 mV/s and the arrows indicate the potential scan directions.

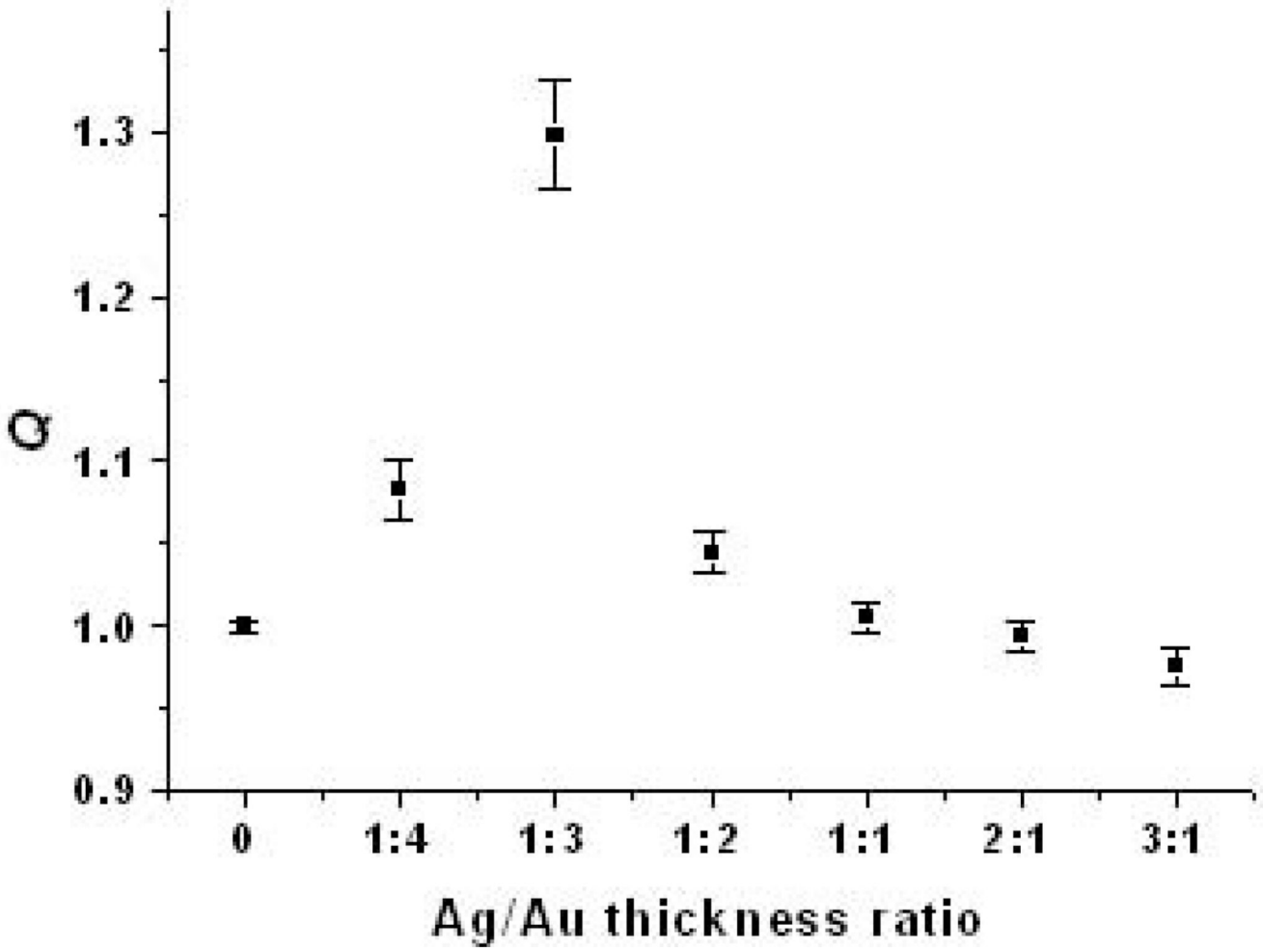

Figure 3.
Correlation of the SPR signal enhancement coefficient *Q* versus the Ag/Au thickness ratio. At least three replicate measurements were made for each thickness to compute the error bars.

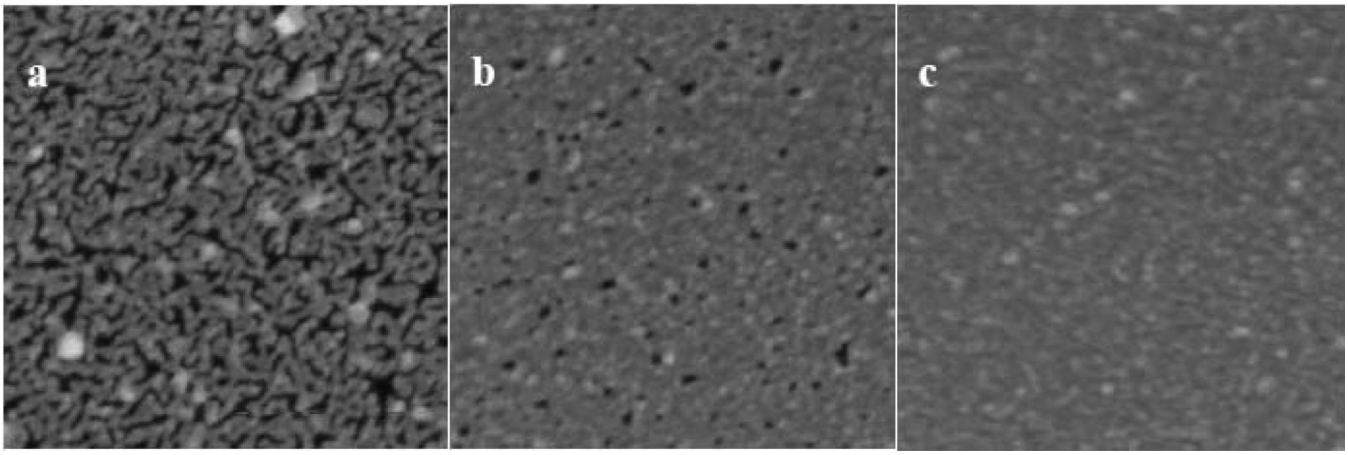

Figure 4.
SEM images of 1×1 μm^2 Ag films with different thickness: 10.0 nm (a), 12.5 nm (b), and 16.7 nm (c).

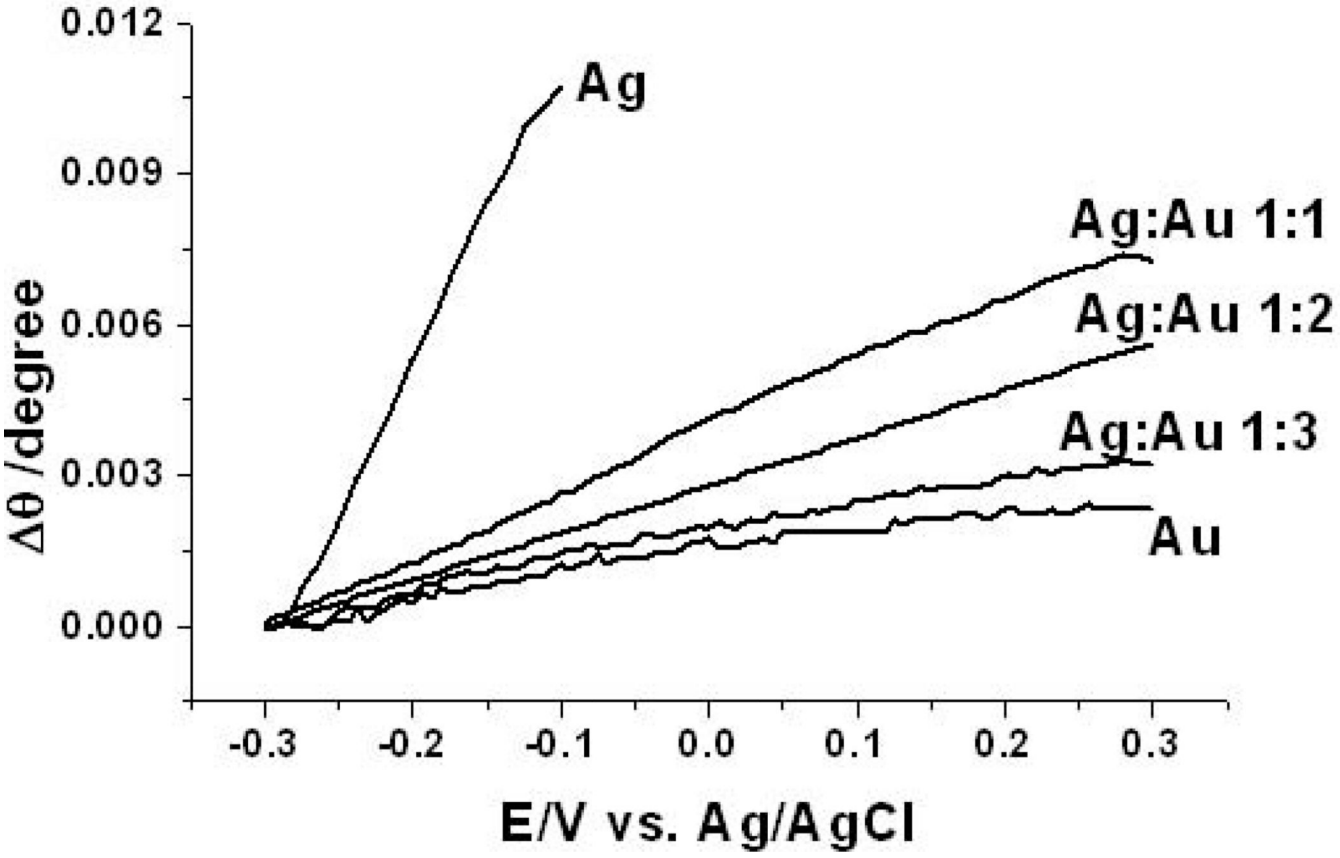

Figure 5.
SPR dip-potential diagrams acquired in 0.1 M H_2SO_4 at Ag/Au films of various thickness ratios. The linear scan rate was 50 mV/s.

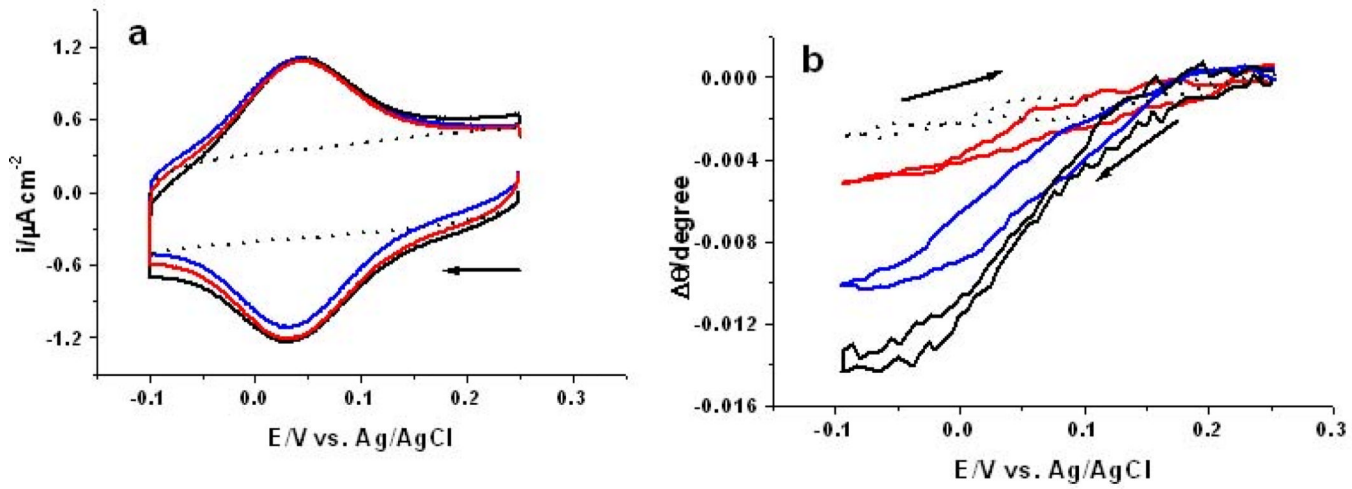

Figure 6.

Cyclic voltammograms (a) and the simultaneous SPR dip shifts (b) with cyt c immobilized onto a MUA SAM preformed onto a pure Au film (red curves), a bilayered Ag/Au film with a thickness ratio of 1/3 (blue curves), and a bilayered film with a ratio of 1/2 (solid black curves). The same measurements were also conducted at a MUA-SAM-covered Au film without cyt *c* (dotted black curves). The scan rate was 50 mV/s and the electrolyte solution was a 50 mM phosphate solution. Arrows indicate the scan directions.